

Statistical mechanics of charged polymers in electrolyte solutions: A lattice field theory approach

Stefan Tsonchev and Rob D. Coalson

Department of Chemistry, University of Pittsburgh, Pittsburgh, Pennsylvania 15260

Anthony Duncan

Department of Physics, University of Pittsburgh, Pittsburgh, Pennsylvania 15260

(Received 25 February 1999)

The lattice field theory approach to the statistical mechanics of a classical Coulomb gas [R.D. Coalson and A. Duncan, *J. Chem. Phys.* **97**, 5653 (1992)] is generalized to include charged polymer chains. Saddle-point analysis is done on the functional integral representing the partition function of the full system. Mean-field level analysis requires extremization of a real-valued functional which possesses a single minimum, thus guaranteeing a unique solution. The full mean-field equations for such a coupled system are derived, as well as the leading (one-loop) fluctuation corrections. Two different numerical real-space lattice procedures are developed to implement the generalized theory; these are applied to the problem of a charged polymer confined to a spherical cavity in an electrolyte solution. The results provide insight into the physics of confined polyelectrolytes. [S1063-651X(99)10709-8]

PACS number(s): 36.20.Ey

I. INTRODUCTION

In a recent series of papers, the application of lattice field theory (LFT) techniques [1–5] to systems of mobile polar ions interacting with immobile macroions has led to a calculational framework for extracting free energies, ionic concentrations, electrostatic potentials, and other physical properties. This formalism, which relies on a Hubbard-Stratonovich transformation of a functional integral representation of the grand canonical partition function, has a number of antecedents in the literature [6–10]. In the generalization introduced in Ref. [1], we were able to obtain accurate results at the mean-field level, *with precisely computable corrections indicating the level of accuracy of the mean-field results*, for systems characterized by arbitrary ionic concentration and macromolecular shape and charge. Reference [1] focused on interactions between charged spherical colloid particles (polyballs) in electrolyte solutions. In a subsequent paper, a liquid phase assembly of many interacting polyballs was studied [2]. The formalism of Ref. [1] has been extended to include effects of a spatially variable dielectric profile [3], the finite size of the simple mobile ions forming the electrolyte [4], and the presence of mobile dipoles in the gas (solution) [5]. The objective of the present paper is to extend the LFT approach to address the statistical mechanics of a gas of mobile charged ions to a system in which mobile charged polymer chains are also present and interacting electrostatically with the mobile ions.

In Sec. II we briefly review the functional integral representation (and lattice field theory discretization thereof) for the grand canonical partition function introduced in Ref. [1]. In Sec. III the formalism is extended to include charged polymer chains. The mean-field level solution of the full system (ions plus polymers) is then presented in Sec. IV. Our results are similar to, but do not fully agree with some recent work of Borukhov *et al.* [11]. In Sec. V we justify the contour deformation introduced in Sec. IV to extract the leading saddle-point (or mean-field theory) equations of the full ion-

polymer system by deriving a general convexity theorem for the mean-field free energy. An explicit expression is also derived for the leading post-mean-field corrections due to the fluctuations around the saddle-point fields. This means that a precise estimate of the error in the mean-field theory is in principle possible even in systems of coupled ions and charged polymer chains. Some simple illustrative applications of the mean-field results of Sec. IV to systems possessing spherical symmetry, for which the problem can be reduced to the minimization of a one-dimensional functional, are described in Sec. VI. The same systems are treated in Sec. VII by solving the mean-field equations on a three-dimensional lattice, an approach which can be used to study systems of arbitrary shape and symmetry. Section VIII summarizes our results and indicates areas for further research.

II. FUNCTIONAL FORMALISM AND LATTICE FIELD THEORY FOR IONIC SYSTEMS

A simple functional integral representation for the grand canonical partition function of a system of mobile ions with electric charge density $\rho(\vec{r})$ is obtained by rewriting the electrostatic potential energy of the system via a standard functional identity:

$$\begin{aligned} & \exp\left[-\frac{\beta}{2\epsilon}\int d\vec{r}d\vec{r}'\frac{\rho(\vec{r})\rho(\vec{r}')}{|\vec{r}-\vec{r}'|}\right] \\ &= C\int D\chi\exp\left[\frac{\epsilon}{8\pi\beta}\int\chi\Delta\chi d\vec{r}+i\int\chi(\vec{r})\rho(\vec{r})d\vec{r}\right]. \end{aligned} \quad (1)$$

Here C is an irrelevant constant (independent of ρ) which will be neglected from now on, and the charges are immersed in a medium of dielectric constant ϵ [12] at inverse temperature $\beta=1/kT$. For a system containing positive and negative mobile ions the charge density is

$$\rho(\vec{r}) = e \sum_k \delta(\vec{r} - \vec{r}_k^+) - e \sum_l \delta(\vec{r} - \vec{r}_l^-). \quad (2)$$

The effect of the transformation induced by Eq. (1) is twofold. First, the long-range Coulomb potential (which makes the direct simulation of such systems by molecular dynamics extremely difficult) has been replaced by a local Laplacian operator. Second, the nonlinear pairwise coupling of the charged ions has been replaced by a linear coupling term where the ions interact only with the auxiliary field. Consequently, for a fixed χ field, the statistical mechanics of the ionic gas is elementary. Introducing chemical potentials μ_{\pm} for the positive and negative ions, the sum of the factor $\exp(i\int \chi(\vec{r})\rho(\vec{r})d\vec{r})$ over ion numbers and positions can be explicitly performed:

$$\begin{aligned} & \sum_{n_k, n_l} \frac{1}{n_k!} \frac{1}{n_l!} \int \prod \frac{d\vec{r}_k}{\lambda_+^3} \frac{d\vec{r}_l}{\lambda_-^3} \exp \left[ie \sum_k \chi(\vec{r}_k) - ie \sum_l \chi(\vec{r}_l) \right. \\ & \quad \left. + \beta(\mu_+ n_k + \mu_- n_l) \right] \\ & = \exp \left[e^{\beta\mu_+} \int \frac{d\vec{r}}{\lambda_+^3} e^{ie\chi} + e^{\beta\mu_-} \int \frac{d\vec{r}}{\lambda_-^3} e^{-ie\chi} \right], \quad (3) \end{aligned}$$

where λ_{\pm} are thermal deBroglie wavelengths for the ions. Inserting this result in the complete expression for the Boltzmann weight (1), the full grand canonical partition function becomes

$$\begin{aligned} Z_{GC} = & \int D\chi \exp \left[\frac{\beta\epsilon}{8\pi} \int \chi \Delta \chi d\vec{r} + e^{\beta\mu_+} \int e^{ie\beta\chi} d\vec{r} / \lambda_+^3 \right. \\ & \left. + e^{\beta\mu_-} \int e^{-ie\beta\chi} d\vec{r} / \lambda_-^3 \right], \quad (4) \end{aligned}$$

where we have rescaled the auxiliary field $\chi \rightarrow \beta\chi$. Various generalizations of this expression [1,3–6,9], have been discussed elsewhere and will not be treated here. For example, the inclusion of a single particle potential $V(\vec{r})$ acting on the ions can be effected simply by the replacement $e^{\pm ie\beta\chi} \rightarrow e^{\pm ie\beta\chi - V}$ in Eq. (4). Such a potential can be used (for example) to exclude the ions from certain regions of space.

The functional integration indicated in Eq. (4) may be made well defined by discretizing the system on a cubical lattice defined by lattice points $\vec{r} = a_l(n_x, n_y, n_z)$, where a_l is a lattice spacing taken small in comparison to the length scales over which the field χ varies substantially, and n_x, n_y, n_z are integers, $0 \leq n_x, n_y, n_z \leq L-1$, for a $L \times L \times L$ lattice. We shall restrict our calculations to systems with zero total electric charge, where the fixed charges are screened by the mobile ones and the fields fall exponentially far from the sources, so finite volume effects go to zero rapidly as the lattice size La_l is increased. With these notations, the lattice version of the transformed partition sum (4) becomes

$$\begin{aligned} Z_{GC} = & \int \prod_n d\chi_n \exp \left\{ \frac{\alpha}{2} \sum_{nm} \chi_n \Delta_{nm} \chi_m + \gamma_+ \sum_n e^{ie\beta\chi_n} \right. \\ & \left. + \gamma_- \sum_n e^{-ie\beta\chi_n} \right\}. \quad (5) \end{aligned}$$

Here Δ_{nm} is the discrete lattice Laplacian operator, which may be regarded as a $L^3 \times L^3$ matrix (see Ref. [1]). The dimensionless constants $\alpha \equiv a_l \beta \epsilon / 4\pi$, $\gamma_{\pm} \equiv e^{\beta\mu_{\pm}} (a_l / \lambda_{\pm})^3$ have been introduced to simplify the notation. In Eq. (5), Δ now represents the discrete lattice gradient (nearest-neighbor difference operator), with e the electronic charge and a_l the lattice spacing.

III. FUNCTIONAL FORMALISM FOR CHARGED POLYMER CHAINS

The path integral representation of a polymer chain [13,14] is well known. We shall show below that for a system consisting of many monomers the leading behavior is determined simply by the total length M (=total number of monomers) of all chains and not by the connectivity or number of the separate chains. Thus the configuration of the polymer chain(s) can be represented by a single function $\vec{x}(s)$, where the dimensionless path length variable $0 \leq s \leq M$. If the typical monomer separation is a_p (the Kuhn length [13]), the partition sum for such a system may be written

$$Z_{pol} = \int D\vec{x}(s) \exp \left[-\frac{3}{2a_p^2} \int_0^M ds \dot{\vec{x}}^2(s) - \frac{\lambda}{2} \int \phi_p(\vec{r})^2 d\vec{r} \right], \quad (6)$$

$$\phi_p(\vec{r}) = \int ds \delta(\vec{r} - \vec{x}(s)). \quad (7)$$

The field ϕ_p is the spatial monomer density and the term involving $\lambda \int \phi_p^2 d\vec{r}$ prevents the monomers from overlapping with each other, $\lambda \geq 0$ being a measure of monomer excluded volume. As discussed at the end of Sec. IV, $\lambda \approx B_2 \approx \sigma^3$, where B_2 is the second virial coefficient, which goes approximately as the monomer volume (i.e., σ is the effective hard-sphere radius of a monomer) [15]. For simplicity we shall assume initially that the polymer charge density is uniform along the polymer chains, with each monomer carrying a net charge of $-pe$ [11] [the generalization to varying monomer charge would simply result in an effective Schrödinger Hamiltonian with a time-dependent potential (see the discussion below)]. The negative sign indicates that we have taken the polymer chain to be negatively charged, as a consequence of dissociation of positively charged counterions. This means that Eq. (2) for the total charge density now becomes [16]

$$\rho(\vec{r}) = e \sum_k \delta(\vec{r} - \vec{r}_k^+) - e \sum_l \delta(\vec{r} - \vec{r}_l^-) - pe \phi_p(\vec{r}). \quad (8)$$

Repeating the argument leading from Eqs. (2) to (4) we now find the following expression for the full partition function of the system:

$$\begin{aligned}
Z = & \int D\chi D\phi_p D\vec{x}(s) \exp\left[\frac{\beta\epsilon}{8\pi} \int \chi \Delta \chi d\vec{r} - \frac{3}{2a_p^2} \int_0^M ds \dot{\vec{x}}^2(s)\right. \\
& - \frac{\lambda}{2} \int \phi_p(\vec{r})^2 d\vec{r} + e^{\beta\mu_+} \int e^{ie\beta\chi} d\vec{r} / \lambda_+^3 \\
& \left. + e^{\beta\mu_-} \int e^{-ie\beta\chi} d\vec{r} / \lambda_-^3 - ipe\beta \int \chi(\vec{r}) \phi_p(\vec{r}) d\vec{r}\right]. \quad (9)
\end{aligned}$$

The integration over polymer configurations can now be replaced by an equivalent Schrödinger Hamiltonian problem. To facilitate this, linearize the dependence on the monomer density ϕ_p by introducing a second auxiliary field

$$\begin{aligned}
\exp\left[-\frac{\lambda}{2} \int \phi_p^2 d\vec{r}\right] = & \int D\omega \exp\left[-\frac{\lambda}{2} \int \omega^2 d\vec{r}\right. \\
& \left. - i\lambda \int \omega(\vec{r}) \phi_p(\vec{r}) d\vec{r}\right]. \quad (10)
\end{aligned}$$

Introducing this representation into Eq. (9) and using Eq. (7), one finds

$$\begin{aligned}
Z = & \int D\chi(\vec{r}) D\omega(\vec{r}) \exp\left[\frac{\beta\epsilon}{8\pi} \int \chi \Delta \chi d\vec{r} - \frac{\lambda}{2} \int \omega(\vec{r})^2 d\vec{r}\right. \\
& \left. + c_+ \int e^{ie\beta\chi} d\vec{r} + c_- \int e^{-ie\beta\chi} d\vec{r}\right] Z_{\text{Schr}}(\chi, \omega) \quad (11)
\end{aligned}$$

with $c_{\pm} = e^{\beta\mu_{\pm}} / \lambda_{\pm}^3$, and

$$\begin{aligned}
Z_{\text{Schr}}(\chi, \omega) \equiv & \int D\vec{x}(s) \exp\left[-\frac{3}{2a_p^2} \int_0^M ds \dot{\vec{x}}^2(s)\right. \\
& \left. - ipe\beta \int ds \chi(\vec{x}(s)) - i\lambda \int ds \omega(\vec{x}(s))\right] \quad (12)
\end{aligned}$$

defines a functional which is just the Feynman path integral for the imaginary time evolution of a particle of mass $3/a_p^2$ in an imaginary potential $i(pe\beta\chi + \lambda\omega)$. In fact, we shall show below that the functional integral (11) over χ and ω can be rerouted through a complex saddle point at $\chi = -i\chi_c$ and $\omega = -i\omega_c$ where χ_c and ω_c are purely *real*, so that the evaluation of $Z_{\text{Schr}}(\chi, \omega)$ at the saddle reduces to a completely conventional three-dimensional Schrödinger Hamiltonian problem—namely, the computation of matrix elements of e^{-HT} where the Euclidean time extent of the evolution is just $T = M$ and

$$H \equiv -\frac{a_p^2}{6} \nabla^2 + \lambda\omega_c(\vec{r}) + \beta pe\chi_c(\vec{r}). \quad (13)$$

For large M , any matrix element of e^{-HT} has the asymptotic form

$$\ln(\langle \dots | e^{-HM} | \dots \rangle) \approx -ME_0 + O(1)$$

where E_0 is the ground state eigenvalue of the Hamiltonian H [17]. Different boundary conditions (periodic, open, etc.)

imposed at the ends of the polymer chain (or even a finite but fixed number of splits in the chain) correspond to the choice of different initial and final states in the above formula, contribute to the $O(1)$ edge correction, and are subdominant for large M .

IV. MEAN-FIELD (SADDLE-POINT APPROXIMATION) THEORY OF COUPLED IONIC-POLYMER SYSTEM

The equations determining the saddle-point configuration fields χ_c, ω_c are obtained by setting the variational derivative of the exponent in the full functional integral (11) to zero. After rotating the fields to the negative imaginary axis (the need for this rotation will be justified below when we discuss the fluctuation corrections), this exponent becomes

$$\begin{aligned}
F = & \int d\vec{r} \left\{ \frac{\beta\epsilon}{8\pi} |\nabla \chi_c|^2 + \frac{\lambda}{2} \omega_c^2 + c_+ e^{\beta e \chi_c} + c_- e^{-\beta e \chi_c} \right\} \\
& - ME_0(\chi_c, \omega_c). \quad (14)
\end{aligned}$$

The functional derivatives determining the saddle-point solution are then

$$\frac{\delta E_0}{\delta \chi_c(\vec{r})} = \beta pe |\Psi_0(\vec{r})|^2, \quad (15)$$

$$\frac{\delta E_0}{\delta \omega_c(\vec{r})} = \lambda |\Psi_0(\vec{r})|^2, \quad (16)$$

$$\begin{aligned}
\frac{1}{\beta e} \frac{\delta F}{\delta \chi_c(\vec{r})} = & -\frac{\epsilon}{4\pi e} \nabla^2 \chi_c(\vec{r}) + c_+ e^{\beta e \chi_c(\vec{r})} - c_- e^{-\beta e \chi_c(\vec{r})} \\
& - Mp |\Psi_0(\vec{r})|^2 = 0, \quad (17)
\end{aligned}$$

$$\frac{1}{\lambda} \frac{\delta F}{\delta \omega_c(\vec{r})} = \omega_c(\vec{r}) - M |\Psi_0(\vec{r})|^2 = 0. \quad (18)$$

Here the wave function $\Psi_0(\vec{r})$ is assumed unit normalized:

$$\int |\Psi_0(\vec{r})|^2 d\vec{r} = 1. \quad (19)$$

Using Eq. (18), the auxiliary field ω_c may be eliminated completely, leaving the pair of coupled nonlinear equations as the complete mean-field solution to the full interacting ion-charged polymer problem:

$$\frac{\epsilon}{4\pi e} \nabla^2 \chi_c(\vec{r}) = c_+ e^{\beta e \chi_c(\vec{r})} - c_- e^{-\beta e \chi_c(\vec{r})} - Mp |\Psi_0(\vec{r})|^2, \quad (20)$$

$$\begin{aligned}
\frac{a_p^2}{6} \nabla^2 \Psi_0(\vec{r}) = & \lambda M |\Psi_0|^2 \Psi_0(\vec{r}) + \beta pe \chi_c(\vec{r}) \Psi_0(\vec{r}) \\
& - E_0 \Psi_0(\vec{r}). \quad (21)
\end{aligned}$$

As mentioned previously, the inclusion of single particle potentials, which can be used to enforce exclusion regions for either the ions or the monomers, is straightforward. Using

the notation $V_c(\vec{r})$ and $V_m(\vec{r})$ for potential fields acting on the mobile ions and monomers, respectively, Eqs. (20), (21) become

$$\frac{\epsilon}{4\pi e} \nabla^2 \chi_c(\vec{r}) = c_+ e^{\beta e \chi_c(\vec{r}) - V_c(\vec{r})} - c_- e^{-\beta e \chi_c(\vec{r}) - V_c(\vec{r})} - Mp |\Psi_0(\vec{r})|^2, \quad (22)$$

$$\frac{a_p^2}{6} \nabla^2 \Psi_0(\vec{r}) = \lambda M |\Psi_0|^2 \Psi_0(\vec{r}) + \beta p e \chi_c(\vec{r}) \Psi_0(\vec{r}) - (E_0 - V_m(\vec{r})) \Psi_0(\vec{r}). \quad (23)$$

Recalling that the parameters c_{\pm} are exponentials of the chemical potentials μ_{\pm} for positively and negatively charged ions, the numbers of these ions must be fixed by suitably adjusting c_{\pm} , using the easily derived relations

$$n_{\pm} = c_{\pm} \frac{\partial \ln(Z_{GC})}{\partial c_{\pm}} = c_{\pm} \int e^{\pm \beta e \chi_c - V_c} d\vec{r} \quad (24)$$

while the number density of monomers is given by $M |\Psi_0(\vec{r})|^2$ which clearly integrates to the total number of monomers M . Charge neutrality follows from integrating Eq. (22) over all space (correct either for periodic boundary conditions or for an electric field falling to zero at the system boundaries):

$$0 = \int \nabla^2 \chi_c(\vec{r}) d\vec{r} \Rightarrow 0 = n_+ - n_- - Mp \quad (25)$$

$$\Rightarrow n_+ e = n_- e + Mpe. \quad (26)$$

For systems of spherical symmetry, the equations (22), (23) reduce to a pair of coupled nonlinear ODEs:

$$\eta \frac{d^2 F}{dr^2} = r (\xi_+ e^{F(r)/r - V_c(r)} - \xi_- e^{-F(r)/r - V_c(r)}) - \frac{1}{r} G(r)^2, \quad (27)$$

$$\frac{1}{6} \frac{d^2 G}{dr^2} = \frac{p}{r} F(r) G(r) + \frac{1}{r^2} G(r)^3 - [E_0 - V_m(r)] G(r), \quad (28)$$

where the rescaled radial functions F, G are defined as

$$F(r) = \beta e r \chi_c(r), \quad (29)$$

$$G(r) = \sqrt{\lambda M} r \Psi_0(r). \quad (30)$$

The radial variable in Eqs. (27), (28) is measured in units of the monomer size a_p , and we have defined dimensionless variables

$$\eta = \frac{\lambda \epsilon}{4\pi \beta p e^2 a_p^2}, \quad (31)$$

$$\xi_{\pm} = \frac{\lambda c_{\pm}}{p}. \quad (32)$$

In terms of these new variables the charge and number density constraints (24)—(26) become

$$\xi_{\pm} \int r^2 e^{\pm F(r)/r - V_c(r)} dr = \frac{\lambda}{4\pi p a_p^3} n_{\pm}, \quad (33)$$

$$\int G(r)^2 dr = \frac{\lambda}{4\pi a_p^3} M = \frac{\lambda}{4\pi a_p^3 p} (n_+ - n_-). \quad (34)$$

In fact, we shall show below that the solution of the coupled nonlinear equations (27),(28) is most readily accomplished by returning to the free energy expression (14), which represents a functional of two scalar fields χ_c, ω_c . This functional will be shown to be convex and bounded below, with a unique minimum at the field values satisfying Eqs. (27),(28).

For nonspherically symmetric systems, a practical approach is again provided by the lattice field theory discretization of Ref. [1]. The inclusion of the polymer terms in Eq. (5) is quite straightforward—discretizing Eq. (11), we obtain (setting the single particle potentials V_c, V_m to zero for simplicity)

$$Z = \int \prod_{\vec{n}} d\chi_{\vec{n}} d\omega_{\vec{n}} \exp \left\{ \frac{\alpha}{2} \sum_{nm} \chi_{\vec{n}} \Delta_{nm} \chi_{\vec{m}} - \frac{\lambda}{2} a_l^3 \sum_{\vec{n}} \omega_{\vec{n}}^2 + \gamma_+ \sum_{\vec{n}} e^{ie\beta \chi_{\vec{n}}} + \gamma_- \sum_{\vec{n}} e^{-ie\beta \chi_{\vec{n}}} - ME_0(\chi_{\vec{n}}, \omega_{\vec{n}}) \right\}, \quad (35)$$

where E_0 is the ground state energy of the associated discrete Hamiltonian matrix

$$H_{mn}^{\vec{r}} = -\frac{a_p^2}{6a_l^2} \Delta_{mn}^{\vec{r}} + i\lambda \omega_{\vec{n}}^{\vec{r}} + i\beta p e \chi_{\vec{n}}^{\vec{r}}. \quad (36)$$

Of course, at the complex saddle point of the integral (35), $\chi = -i\chi_c$ and $\omega = -i\omega_c$ with χ_c, ω_c real fields, so the Hamiltonian matrix (36) is real symmetric, with well-defined real ground state energy. After the rotation to the imaginary axis, we find the following expression for the discretized free energy functional [corresponding to the continuum expression given in Eq. (14)]:

$$F = -\frac{\alpha}{2} \sum_{mn} \chi_{\vec{m}} \Delta_{mn} \chi_{\vec{n}} + \frac{\lambda}{2} a_l^3 \sum_{\vec{n}} \omega_{\vec{n}}^2 + \gamma_+ \sum_{\vec{n}} e^{\beta e \chi_{\vec{n}}} + \gamma_- \sum_{\vec{n}} e^{-\beta e \chi_{\vec{n}}} - ME_0(\chi_{\vec{n}}, \omega_{\vec{n}}), \quad (37)$$

where we have dropped the subscript c indicating the saddle-point (mean-field) value for the fields to avoid notational overload. Now the ground state energy, as promised, is a perfectly real number, namely, the lowest eigenvalue of the matrix

$$H_{mn}^{\vec{r}} = -\frac{a_p^2}{6a_l^2} \Delta_{mn}^{\vec{r}} + \lambda \omega_{\vec{n}}^{\vec{r}} + \beta p e \chi_{\vec{n}}^{\vec{r}}. \quad (38)$$

For a long Gaussian polymer chain in a confined region and subjected to an *external* potential $W(\vec{r})$, it is well known [13] that the ground state of the three dimensional Schrödinger operator

$$\hat{H} = -\frac{a_p^2}{6}\nabla^2 + \beta W(\vec{r}) \quad (39)$$

determines the equilibrium properties of the polymer chain. In particular, if $\Psi_0(\vec{r})$ is the unit-normed ground state eigenfunction associated with Hamiltonian (39) (with $\Psi_0=0$ on the confining boundary surface) then $|\Psi_0(\vec{r})|^2$ is the unit normalized monomer density. Equivalently, if there are M monomers in the polymer system then $M|\Psi_0(\vec{r})|^2$ is the number density of monomers in the system. Comparing Eq. (39) to Eqs. (38), (18) above, we see that in our problem there is an *effective* potential

$$W(\vec{r}) = kT\lambda M|\Psi_0(\vec{r})|^2 + pe\chi_c(\vec{r}).$$

Since both terms in this potential are functions (explicitly or implicitly) of Ψ_0 , our effective potential W is evidently a *mean-field* potential. Specifically, the electric potential χ_c depends on the monomer charge density (hence Ψ_0) according to Eq. (20). The other contribution to the effective potential, i.e., $kT\lambda M|\Psi_0(\vec{r})|^2$, is due to short-range excluded volume interactions between monomers. Its origin and form can be understood as follows. Let $U(\vec{r})$ be a short range repulsive potential via which all monomer pairs interact. Then, if there is a distribution $n_m(\vec{r})$ of monomers in the system, the repulsive potential (call this W , suppressing the electrostatic contribution) experienced by a test monomer inserted at point \vec{r} is

$$W(\vec{r}) = \int d\vec{r}' U(\vec{r}-\vec{r}')n_m(\vec{r}') \quad (40)$$

$$\cong n_m(\vec{r}) \int d\vec{r} U(\vec{r}). \quad (41)$$

The second line follows from the first under the assumption that the pair potential U is short range compared to the length scale on which the monomer density n_m varies. Using the connection (noted above) that $M|\Psi_0(\vec{r})|^2 = n_m(\vec{r})$, we immediately identify the parameter λ as

$$\lambda = \beta \int U(\vec{r})d\vec{r}. \quad (42)$$

This can in turn be connected to the second virial coefficient B_2 , which can be used to ascribe an effective ‘‘hard sphere’’ radius σ to the monomer [15]:

$$\beta \int U(\vec{r})d\vec{r} \cong - \int d\vec{r} [e^{-\beta U(\vec{r})} - 1] = 2B_2 \cong 4\pi\sigma^3/3. \quad (43)$$

In this way we can connect λ with the effective size of a monomer.

V. CORRECTIONS TO MEAN-FIELD THEORY— CONVEXITY OF THE FREE ENERGY

In the preceding section we claimed that the functional integral (11) is dominated by a complex saddle point where the fields χ, ω take pure imaginary values $-i\chi_c, -i\omega_c$. To justify this assertion, we need to ensure that the deformation of the contour of the field integrations is such that the integral passes through a proper saddle-point, with a maximum of the real part of the exponent, and that the saddle chosen is the dominant one globally. A rigorous discussion presupposes that the functional integral (11) has been made well defined, say by discretization as in Eq. (35). As a consequence we may be sure that the contour deformation is possible in the first place as a result of the analyticity of $Z_{\text{Schr}} = \text{Tr} e^{-MH(\chi_n^-, \omega_n^-)}$ as a function of the variables χ_n^-, ω_n^- for an arbitrary finite-dimensional matrix H . We remind the reader that the result $Z_{\text{Schr}} = \text{Tr} e^{-MH}$ holds for closed polymer chains but that different boundary conditions induce subdominant edge effects of order $O(1/M)$ for long chains with M monomers [see the discussion following Eq. (13)]. The analyticity of the remaining part of the integrand in Eq. (35) is obvious.

For simplicity we shall temporarily return to continuum notation, although the reader is warned that ultimately the functional integral being discussed must be explicitly defined by a cutoff procedure. Writing

$$\begin{aligned} \chi(\vec{r}) &= -i\chi_c(\vec{r}) + \hat{\chi}(\vec{r}), \\ \omega(\vec{r}) &= -i\omega_c(\vec{r}) + \hat{\omega}(\vec{r}), \end{aligned} \quad (44)$$

we may expand the integrand of the functional integral (11) keeping terms up to second order in the fluctuation fields $\hat{\chi}, \hat{\omega}$:

$$\begin{aligned} Z &= e^F \int D\hat{\chi}(\vec{r})D\hat{\omega}(\vec{r}) \exp \left\{ - \int d\vec{r} \left[\frac{\beta\epsilon}{8\pi} |\vec{\nabla}\hat{\chi}(\vec{r})|^2 \right. \right. \\ &\quad \left. \left. + \frac{\lambda}{2}\hat{\omega}(\vec{r})^2 + \frac{\beta^2 e^2}{2} (c_+ e^{\beta e\chi_c} + c_- e^{-\beta e\chi_c}) \hat{\chi}(\vec{r})^2 \right] \right\} \\ &\quad \times \exp \left\{ -M \int d\vec{r}d\vec{r}' [\lambda\hat{\omega}(\vec{r}) + \beta pe\hat{\chi}(\vec{r})] G_c(\vec{r}, \vec{r}') \right. \\ &\quad \left. \times [\lambda\hat{\omega}(\vec{r}') + \beta pe\hat{\chi}(\vec{r}')] \right\}, \end{aligned} \quad (45)$$

where the prefactor e^F contains the entire mean-field result (14), and the ‘‘one-loop’’ fluctuation corrections to mean-field are contained in the remaining Gaussian functional integral over the fluctuation fields $\hat{\chi}, \hat{\omega}$. The crucial point is that this integral is convergent as a consequence of the positivity of the Green’s function $G_c(\vec{r}, \vec{r}')$ giving the second order variation with $\hat{\chi}, \hat{\omega}$ of the ground state eigenvalue E_0 of the Hermitian Hamiltonian (13). Let $\Psi_n(\vec{r})$ be a complete orthonormal set of eigenfunctions of H , with the corresponding ordered eigenvalues $E_n, E_n \leq E_m$ for $n < m$. Then standard second order perturbation theory gives, as a consequence of Eq. (44),

$$\begin{aligned}
E_0(\chi, \omega) &\simeq E_0(\chi_c, \omega_c) + \int d\vec{r} d\vec{r}' [\lambda \hat{\omega}(\vec{r}) \\
&\quad + \beta p e \hat{\chi}(\vec{r})] G_c(\vec{r}, \vec{r}') [\lambda \hat{\omega}(\vec{r}') + \beta p e \hat{\chi}(\vec{r}')], \\
G_c(\vec{r}, \vec{r}') &= \Psi_0(\vec{r}) \Psi_0(\vec{r}') \sum_{n \neq 0} \frac{\Psi_n(\vec{r}) \Psi_n(\vec{r}')}{E_n - E_0} \quad (46)
\end{aligned}$$

through terms of second order in the fluctuation fields. Note that the first order perturbation shift in E_0 is canceled at the saddle-point by the first order variation in the exponent in Eq. (11). Furthermore, the positivity (strictly speaking, positive semidefiniteness) of G_c is manifest. To see this, note that a necessary and sufficient condition for G_c to be positive semidefinite is

$$\int d\vec{r} \int d\vec{r}' f(\vec{r}) G_c(\vec{r}, \vec{r}') f(\vec{r}') \geq 0 \quad (47)$$

for any function $f(\vec{r})$. Using the definition given in Eq. (46),

$$\begin{aligned}
&\int d\vec{r} \int d\vec{r}' f(\vec{r}) G_c(\vec{r}, \vec{r}') f(\vec{r}') \\
&= \sum_{n \neq 0} \frac{\left[\int d\vec{r} \Psi_0(\vec{r}) f(\vec{r}) \Psi_n(\vec{r}) \right]^2}{E_n - E_0}. \quad (48)
\end{aligned}$$

Since the denominator of each term on the right-hand side is positive and the numerator is non-negative the condition for positive semidefiniteness (47) is satisfied.

It should be emphasized that the positivity of the full fluctuation kernel in Eq. (45) holds for arbitrary real fields χ_c, ω_c —it is not essential that they satisfy the saddle-point equations (20), (21) (although we shall, of course, eventually demand that they do). The value of this observation is that it is equivalent to a statement of convexity of the free energy functional $F(\chi_c, \omega_c)$ in Eq. (14) for arbitrary values of its

field arguments, as the exponent in the fluctuation integral (45) is essentially the second functional derivative of F . The functional $F(\chi_c, \omega_c)$ is clearly bounded below [as the lowest eigenvalue of H in Eq. (13) can grow at most linearly with χ_c or ω_c]. If it is everywhere convex, it must have a *unique* minimum at exactly the field values χ_c, ω_c satisfying Eqs. (20), (21). Thus the stable minimization procedures employed in Ref. [1] for solving the lattice field theory of systems of polyballs and mobile ions are guaranteed to work here also, in the presence of long charged polymer chains, provided an efficient numerical technique is employed.

We now return to the task of evaluating the Gaussian fluctuation integral (45). It is convenient to change the field integration variables by replacing the excluded volume field $\hat{\omega}(\vec{r})$ with the linear combination

$$\sigma(\vec{r}) \equiv \lambda \hat{\omega}(\vec{r}) + \beta p e \hat{\chi}(\vec{r}) \quad (49)$$

so that the fluctuation integral in Eq. (45) becomes

$$\begin{aligned}
e^{F_1} &= \int D\hat{\chi}(\vec{r}) D\sigma(\vec{r}) \exp \left[- \int d\vec{r} \left\{ \frac{\beta \epsilon}{8\pi} |\vec{\nabla} \hat{\chi}(\vec{r})|^2 \right. \right. \\
&\quad + \frac{1}{2\lambda} [\sigma(\vec{r}) - \beta p e \hat{\chi}(\vec{r})]^2 \\
&\quad \left. \left. + \frac{\beta^2 e^2}{2} (c_+ e^{\beta e \chi_c} + c_- e^{-\beta e \chi_c}) \hat{\chi}(\vec{r})^2 \right\} \right] \\
&\quad \times \exp \left[-M \int d\vec{r} d\vec{r}' \sigma(\vec{r}) G_c(\vec{r}, \vec{r}') \sigma(\vec{r}') \right] \quad (50)
\end{aligned}$$

whence

$$F_1 = -\frac{1}{2} \ln \text{Det} K, \quad (51)$$

where K is the kernel

$$K = \begin{pmatrix} -\frac{\beta \epsilon}{8\pi} \Delta + \frac{\beta^2 p^2 e^2}{2\lambda} + \frac{\beta^2 e^2}{2} (c_+ e^{\beta e \chi_c} + c_- e^{-\beta e \chi_c}) & -\frac{\beta p e}{2\lambda} \\ -\frac{\beta p e}{2\lambda} & M G_c + \frac{1}{2\lambda} \end{pmatrix}.$$

This determinant must be rendered well defined by an explicit cutoff procedure, such as the lattice. On a lattice with N points, we then have the problem of evaluating a $2N \times 2N$ determinant. If the polymer is restricted to a subregion of N_p points, the lower right hand $N \times N$ block in K is non-sparse only in a $N_p \times N_p$ subblock of the kernel G_c . The evaluation of G_c is facilitated by the observation that

$$\sum_{n \neq 0} \frac{\Psi_n(\vec{r}) \Psi_n(\vec{r}')}{E_n - E_0} = \lim_{\eta \rightarrow 0} \left((H - E_0) \frac{1}{(H - E_0)^2 + \eta^2} \right) (\vec{r}, \vec{r}') \quad (52)$$

with the required inversion involving only a sparse matrix $(H - E_0)^2 + \eta^2$.

VI. MEAN-FIELD RESULTS FOR SPHERICALLY SYMMETRIC SYSTEMS

For spherically symmetric systems, the extremization of the functional F in Eq. (14) is much simplified. It is convenient to express all distances in units of the effective monomer size (Kuhn length) a_p , and to define rescaled radial functions $f(r), g(r)$ as follows:

$$f(r) = \beta e \chi_c(r), \quad (53)$$

$$g(r) = r \Psi_0(r). \quad (54)$$

It is also convenient to rescale the auxiliary field ω_c to a dimensionless one, $h(r) \equiv \omega_c(r) a_p^3$. Introducing dimensionless parameters η , ξ_{\pm} , and ζ ,

$$\eta \equiv \frac{\epsilon a_p}{2\beta e^2}, \quad (55)$$

$$\xi_{\pm} \equiv 4\pi c_{\pm} a_p^3, \quad (56)$$

$$\zeta \equiv 4\pi \frac{\lambda}{a_p^3}, \quad (57)$$

the saddle-point functional can be written in terms of a one-dimensional integral

$$F = \int \left\{ \eta \left(\frac{df}{dr} \right)^2 + \frac{1}{2} \zeta h(r)^2 + \xi_+ e^f + \xi_- e^{-f} \right\} r^2 dr - M E_0, \quad (58)$$

where the radial wave function $g(r)$ of the associated Schrödinger Hamiltonian (13) satisfies

$$\frac{1}{6} \frac{d^2 g}{dr^2} = \left(\frac{\zeta}{4\pi} h(r) + p f(r) - E_0 \right) g(r). \quad (59)$$

The rescaled activity coefficients ξ_{\pm} must be constrained by the appropriately rescaled versions of Eq. (33):

$$\xi_{\pm} = \frac{n_{\pm}}{\int e^{\pm f} r^2 dr}. \quad (60)$$

We have devised the following efficient procedure for the minimization of F in Eq. (58). The arguments of the preceding section establish the convexity of F , implying a unique minimum. After discretizing the r variable, the rescaled electrostatic potential function $f(r)$ and polymer density function $h(r)$ become finite arrays which can be updated alternately by the following procedure, which at each step takes us closer to the unique global extremum of F :

(1) Choose a reasonable starting value for the fields f, h .

(2) Define a new field $\sigma(r) \equiv \zeta h(r)/4\pi + p f(r)$, so that E_0 in (58) is the lowest eigenvalue of the operator $H = -\frac{1}{6}(d^2/dr^2) + \sigma(r)$. Once r is discretized, H becomes a tridiagonal matrix. For the rest of the calculation, we minimize with respect to $f(r)$ and $\sigma(r)$.

(3) Minimize F with respect to $\sigma(r)$ for each discrete value of r . This requires a rapid calculation of E_0 as a function of $\sigma(r)$. The ground state eigenvalue of a tridiagonal matrix (indeed, any ordinally located eigenvalue) can be readily extracted by Sturm sequence methods [18], and the functional F minimized quickly with respect to $\sigma(r)$ by golden section bracketing [19]. The latter approach is fool-proof as we have a strictly convex dependence on $\sigma(r)$ for all r .

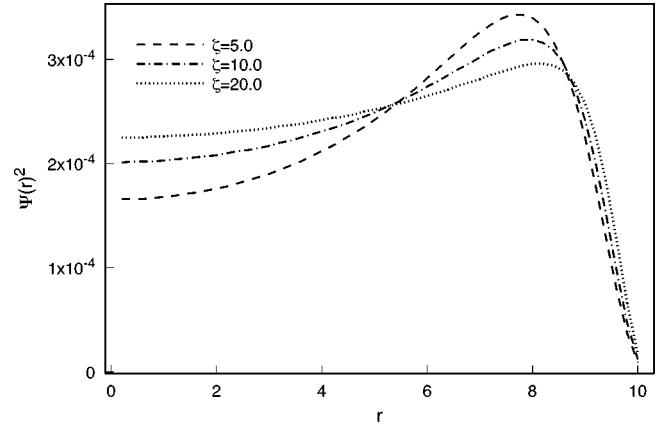


FIG. 1. Monomer distribution for varying ζ .

(4) Minimize F with respect to $f(r)$ for each discrete value of r . This is trivial as the dependence of F on $f(r)$ is explicit.

(5) Iterate until F stabilizes at a minimum to some preassigned tolerance and/or the saddle-point equations are satisfied to a desired degree of accuracy.

This algorithm was applied to a system consisting of a charged polymer with 1000 monomer subunits trapped in a spherical cavity of radius $10a_p$, with each monomer carrying a charge $-0.1e$. The ions ($n_+ = 200$ positive and $n_- = 100$ negative ions) are free to move in a larger spherical region of radius $100a_p$. The parameter η was taken to be unity. The results shown correspond to 1000 iterations, after which the free energy is stabilized to five significant figures (such a run takes a few minutes on a 400 MHz Pentium processor). The effect of variation of the excluded volume parameter ζ on the monomer density $\Psi_0^2(r)$ is shown in Fig. 1. As for the case of the uncharged polymer, increasing the excluded volume parameter results in a flattening of the distribution near the origin. However, in the presence of charge, we now find that (at least for the parameter range studied here) the electrostatic repulsion sufficiently counteracts the tendency of the monomers to crowd into the central region to produce a *dip* in the distribution for small r . The mean-field rescaled electric potential $f(r)$ is nearly constant over this variation of ζ , as shown in Fig. 2 [20,21]. The exponential screening outside the cavity of radius $10a_p$ confining the polymer is evident.

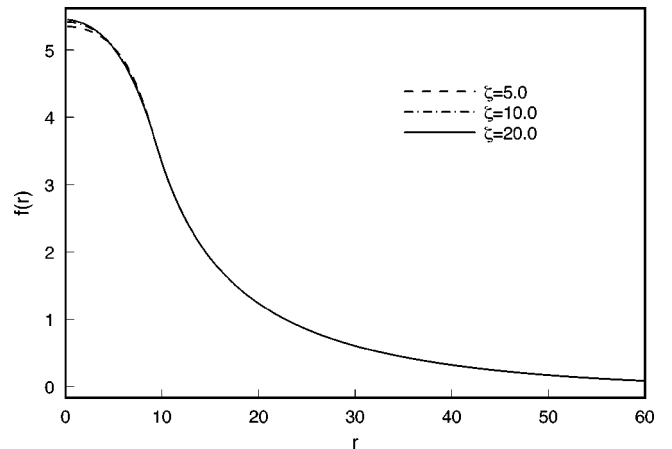
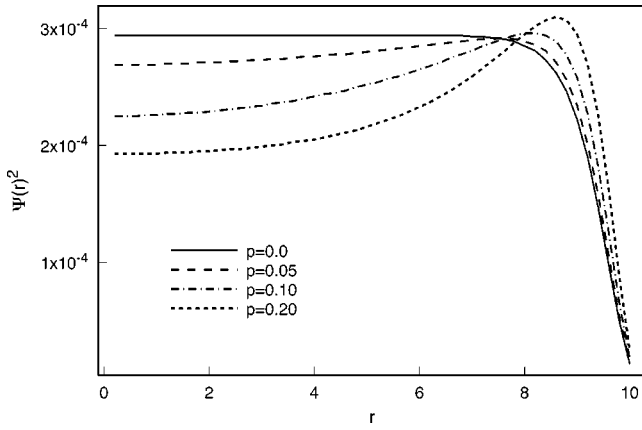


FIG. 2. Electric potential $f(r)$ for varying ζ .

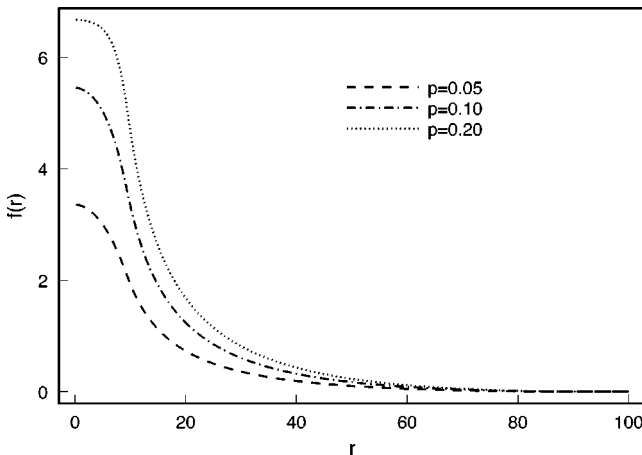
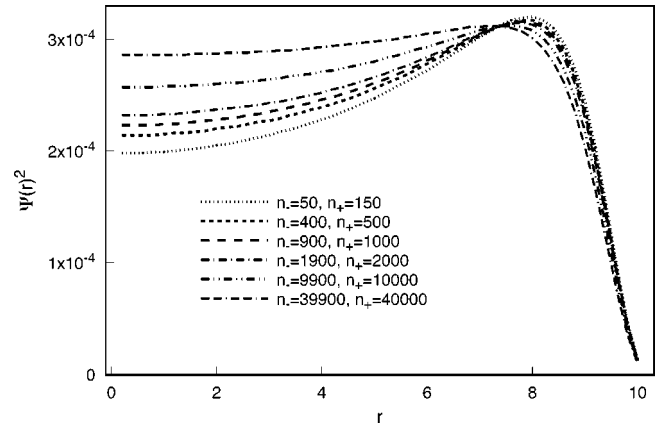
FIG. 3. Monomer distribution for varying p .

The effect of varying monomer charge p (with the excluded volume parameter ζ held fixed at 20.0) is illustrated in Figs. 3 and 4. In particular, as $p \rightarrow 0$ we recover the distinctive flat behavior at small r characteristic of uncharged polymers (Fig. 3). In these plots, the negative ion number is held constant at 100, with the number of positive ions adjusted to give charge neutrality.

Finally, we may also study the effect of varying salt concentrations. Increasing the background ion density results in higher screening of the electrostatic potential, so the effect on the monomer distribution is similar to that obtained by varying the average monomer charge p . In Figs. 5 and 6 we show the monomer distribution and electrostatic potential $f(r)$ for fixed $\zeta=10$ and $p=0.1$, varying the number of negative mobile ions n_- , with $n_+ = n_- + 100$ for charge neutrality.

VII. MEAN-FIELD RESULTS USING THREE-DIMENSIONAL LATTICE FIELD THEORY

In the previous section we showed how the theory developed in this paper can be applied to the problem of a charged polymer confined to a spherical cavity and immersed in an electrolyte solution. We now present the solution of the same problem using three-dimensional (3D) lattice field theory, which does not hinge on special symmetry properties of the system, and thus illustrate a numerical procedure for dealing

FIG. 4. Electric potential $f(r)$ for varying p .FIG. 5. Monomer distribution for varying n_- .

with systems of arbitrary shape and complexity. Colloidal suspensions in polyelectrolyte solutions, which may be useful for a variety of technological applications, such as new optical materials and devices (e.g., narrow-band optical rejection filters, pump-probe laser apparatus, optical display panels, etc. [22,23]), are systems of this type.

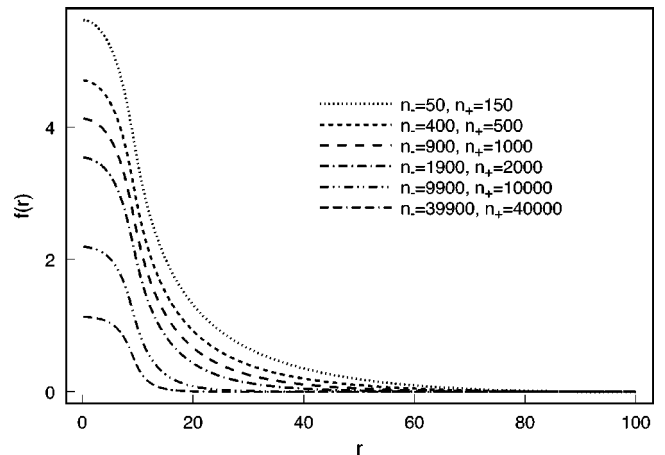
We will solve the discretized versions of equations (22) and (23) simultaneously on a 3D lattice. It is convenient to multiply equation (22) by a_l^3 , where a_l is the lattice spacing, and to rescale according to $f(\vec{r}) \rightarrow \beta e \chi_c(\vec{r})$, $\Psi_0(\vec{r}) \rightarrow a_l^{3/2} \Psi_0(\vec{r})$. Thus, all variables and parameters become dimensionless and the two discretized equations are

$$\alpha \sum_m \Delta_{nm} f_m^- = \gamma_+ e^{f_n^- - V_n^-} - \gamma_- e^{-f_n^- - V_n^-} - M p \Psi_n^2, \quad (61)$$

$$\frac{a_p^2}{6a_l^2} \sum_m \Delta_{nm} \Psi_m^- = \frac{\lambda M}{a_l^3} \Psi_n^2 \Psi_n^- + p f_n^- \Psi_n^- - E_0 \Psi_n^-, \quad (62)$$

where

$$\alpha = \frac{\varepsilon a_l}{4 \pi \beta e^2}, \quad (63)$$

FIG. 6. Electric potential $f(r)$ for varying n_- .

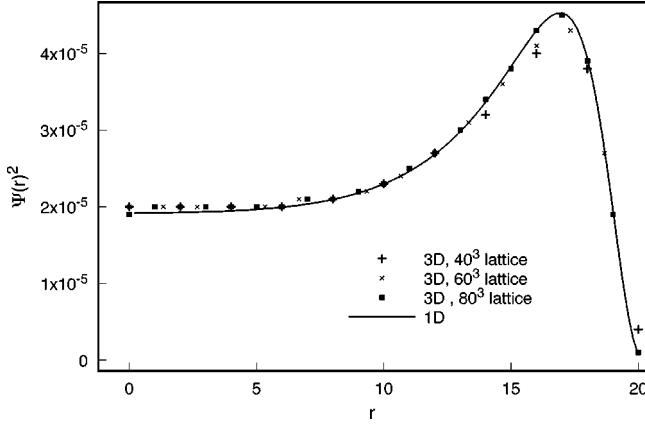


FIG. 7. Monomer distribution for varying lattice size.

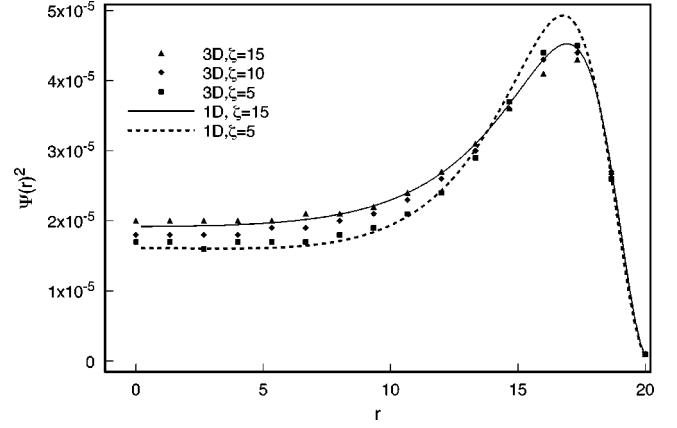
$$\gamma_{\pm} = \frac{n_{\pm}}{\sum_n e^{\pm f_n^-}}, \quad (64)$$

and the wave function is dimensionless and normalized according to

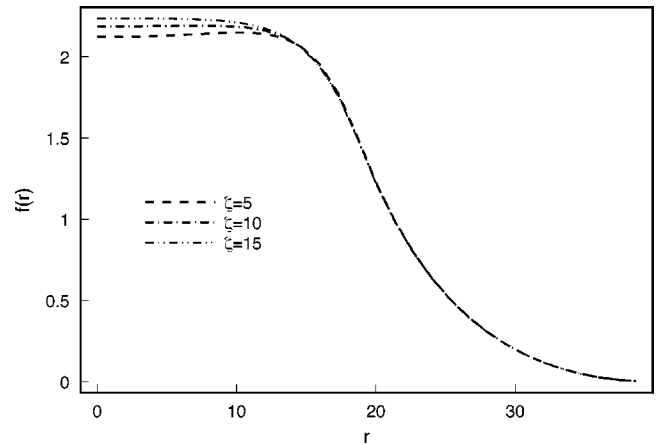
$$\sum_n \Psi_n^2 = 1. \quad (65)$$

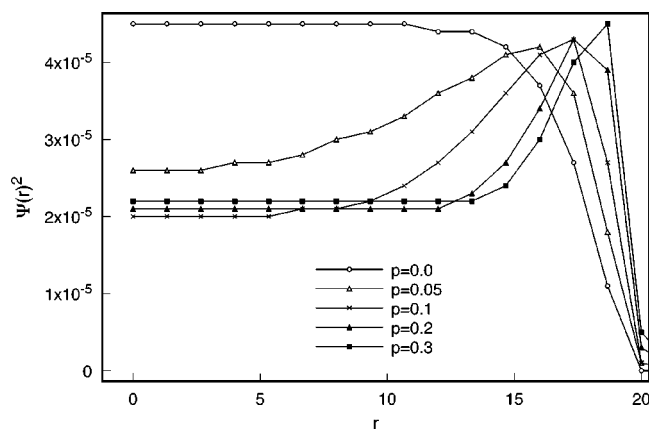
We solve Eqs. (61) and (62) simultaneously using the following procedure. First, Eq. (62) is solved for $f_n^- = 0$ and ignoring the nonlinear (monomer repulsion) term. The resulting Ψ_n^- (wave function for a free particle in a sphere) is given to Eq. (61), which is solved at each lattice point by the Newton-Raphson method. The process is repeated and the coefficients γ_{\pm} are updated after each iteration with the current field, until a predetermined desired accuracy is achieved. Then the resulting f_n^- is fed into Eq. (62) which is solved for a new Ψ_n^- to be given to Eq. (61). Equation (62) is solved to a predetermined desired accuracy by the Lanczos approach, which is appropriate for a large sparse matrix such as the one representing our Hamiltonian. This method of computation is very well suited for implementation on massively parallel platforms which should make it possible to study even very large lattices with this approach. From then on, the potential f_n^- to be given to Eq. (62) for the next iteration is updated slowly by adding a small fraction of the new f_n^- to the old one, obtained from the previous iteration. The same relaxation procedure is used for updating Ψ_n^2 in the nonlinear term of the Schrödinger equation (62). Such a gradual iteration procedure is necessary in order to avoid an unstable bifurcation between two unphysical states (which is commonly encountered when solving nonlinear differential equations), and it converges to the simultaneous solution of the two equations. We have shown above that the functional in Eq. (14) has a unique minimum, the condition for which is given by the two equations, (61) and (62). Therefore, once we have converged to a solution of these two equations, we are guaranteed to have reached the unique mean-field solution of the problem.

We have applied the procedure described above to a system of a negatively charged polymer of 1000 monomer units,

FIG. 8. Monomer distribution for varying ζ .

confined to a spherical cavity of radius $20a_p$, which is immersed in an electrolyte solution confined to a larger sphere of radius $40a_p$. The Kuhn length a_p has been chosen to be 5 Å. To illustrate the stability and accuracy of the procedure, we compare some of the 3D results with the ones obtained through the one-dimensional (1D) calculation of Sec. VI, which are practically exact. In Fig. 7 we show how the 3D results for $\Psi_0^2(\vec{r})$ approach the exact 1D result as the number of the lattice points on the side of the 3D cube containing the system L is increased from 40 to 60 and 80, for the following parameters: $\zeta = 15$, $p = 0.1$, and $n_- = 6$, where n_- is the number of the negative ions in the system, while the number of the positive ions is adjusted so that electroneutrality is preserved, and the relationship between ζ and λ [in Eq. (62)] is given in Eq. (57). The rest of the 3D calculations (the results of which are presented in Figs. 8 through 13) are performed on a cube with 60 lattice points on each side. In Fig. 8 we show the effect of variation of ζ on the probability distribution $\Psi_0^2(\vec{r})$. For comparison we have included two results obtained by the 1D method of Sec. VI. The results are analogous to the ones in Fig. 1. Similarly, the rescaled electrostatic potential $f(\vec{r})$ varies little with ζ , as shown in Fig. 9. In Figs. 10 and 11 we present results for $\Psi_0^2(\vec{r})$ and $f(\vec{r})$ for varying monomer charge p , fixing $\zeta = 15$. In these plots the number of negative ions is $n_- = 6$. And finally, in Figs. 12 and 13 we illustrate the effect of varying the number of im-

FIG. 9. Electric potential $f(r)$ for varying ζ .

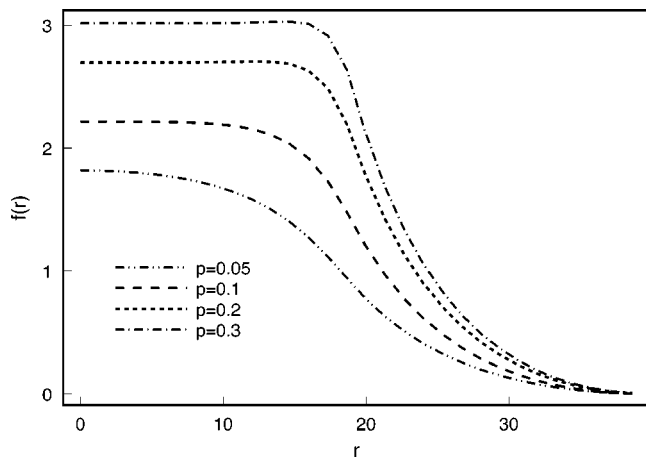
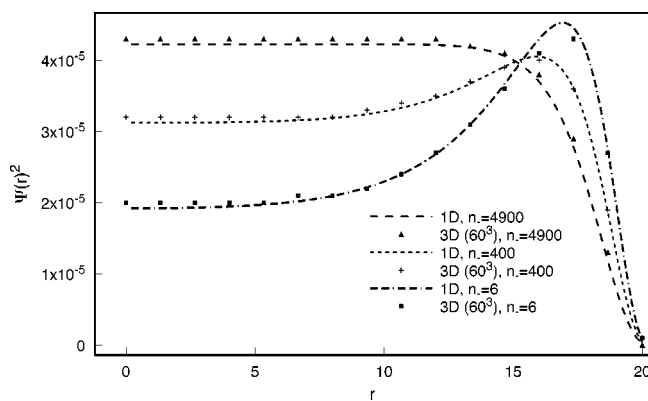
FIG. 10. Monomer distribution for varying p .

purity ions on the monomer distribution and the potential $f(\vec{r})$. Here, again, we compare the 3D results with the ones obtained by the 1D method of Sec. VI. Clearly, the agreement between the two approaches is good.

VIII. DISCUSSION

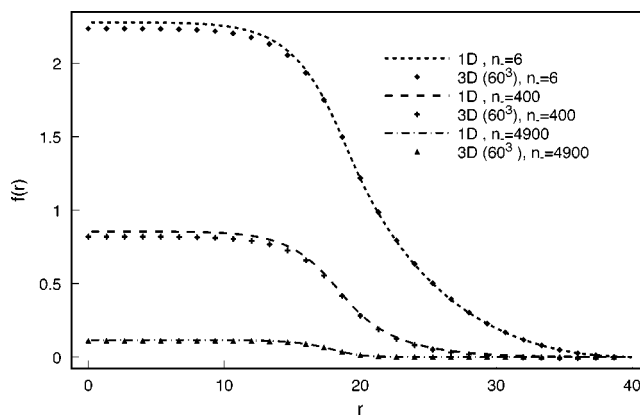
We have derived the mean-field equations for a coupled ionic-polymer system by performing a saddle-point analysis on a functional integral representing the partition function of the system, Eq. (11). This analysis shows that all mean-field level thermodynamical properties are obtained by extremizing an appropriate real-valued functional (14). Moreover, we have shown that the functional (14) possesses a single extremum, which is a minimum, thus guaranteeing a unique solution of the coupled mean-field equations. We have also described two different numerical procedures for finding the mean-field solution, and have applied them to the problem of a charged polymer confined to a spherical cavity and immersed in an electrolyte solution.

Although our calculations were intended as an illustration of the advantages of the approach, they have yielded some interesting insight into the physics of confined polyelectrolytes. It has been suggested that materials consisting of spherical voids imbedded in a polymer gel can be used as “entropic trapping devices,” in which macromolecules (e.g., polymers and DNA) could be trapped and separated [24].

FIG. 11. Electric potential $f(r)$ for varying p .FIG. 12. Monomer distribution for varying n .

Therefore, these materials may have important applications in specific biochemical trapping, or even as microreactors for applications in organic, bioengineering and combinatorial synthesis [24].

It has been hypothesized [25–28] that such trapping is a result of the higher conformational entropy “enjoyed” by the polymer in the large spherical void, as compared to the narrow channels connecting the voids within the gel. Our calculations reveal another important aspect of the trapping phenomenon—namely, from our results it becomes clear that electrostatic interactions also play a very important role in it. From Figs. 3, 5, 10, and 12 it is seen that polymers with high monomer charge p , or in dilute electrolyte solution, have a distribution function with a peak near the edge of the spherical cavity, while polymers with low monomer charge or in concentrated electrolyte solution (where the monomers are highly screened by the impurity ions, thus experiencing weaker electrostatic repulsion from each other), have a more flattened distribution, and are more likely to be found near the center, rather than the edge of the cavity. In addition, highly charged monomers would possess higher energy in the voids, due to the stronger repulsion from each other as they are brought closer together in the folded polymer. Therefore, we expect that polymers with relatively low average monomer charge or in a concentrated electrolyte solution would be easier to trap in spherical voids. Usually the monomer charge is approximately constant, and it is the impurity ion concentration that can be varied in the laboratory. We

FIG. 13. Electric potential $f(r)$ for varying n .

suggest that experiments be performed to investigate polymer trapping dependence on electrolyte concentration. We also expect that the lattice field theory approach to the statistical mechanics of charged polymers in electrolyte solution

which has been developed in the present work will be useful for studying low symmetry systems involving complex liquids, such as colloidal suspensions in polyelectrolyte solutions.

-
- [1] R.D. Coalson and A. Duncan, *J. Chem. Phys.* **97**, 5653 (1992).
- [2] A.M. Walsh and R.D. Coalson, *J. Chem. Phys.* **100**, 1559 (1994).
- [3] N. Ben-Tal and R.D. Coalson, *J. Chem. Phys.* **101**, 5148 (1994).
- [4] R.D. Coalson, A.M. Walsh, A. Duncan, and N. Ben-Tal, *J. Chem. Phys.* **102**, 4584 (1995).
- [5] R.D. Coalson and A. Duncan, *J. Phys. Chem.* **100**, 2612 (1996).
- [6] S.F. Edwards, *Philos. Mag.* **4**, 1171 (1959).
- [7] A.L. Kholodenko and A.L. Beyerlein, *Phys. Rev. A* **34**, 3309 (1986); R. Varoqui, *J. Phys. II* **3**, 1097 (1993).
- [8] A. Duncan and R. Mawhinney, *Phys. Rev. D* **43**, 554 (1991).
- [9] R. Podgornik and B. Zeks, *J. Chem. Soc., Faraday Trans. 2* **84**, 611 (1988); R. Podgornik, *J. Phys. A* **23**, 275 (1990).
- [10] R. Podgornik, *J. Phys. Chem.* **96**, 884 (1992); R. Podgornik, *J. Phys. Chem.* **95**, 5249 (1991).
- [11] I. Borukhov, D. Andelman, and H. Orland, *Eur. Phys. J. B* **5**, 869 (1998).
- [12] It was shown in Ref. [3] that an arbitrary dielectric profile $\epsilon(\vec{r})$ can be incorporated into the LFT formalism in a straightforward way. For simplicity, we consider only the prototypical case of constant ϵ here.
- [13] M. Doi and S.F. Edwards, *The Theory of Polymer Dynamics* (Oxford University Press, Oxford, 1986).
- [14] F.W. Wiegel, *Introduction to Path-Integral Methods in Physics and Polymer Science* (World Scientific, Singapore, 1986).
- [15] D.A. McQuarrie, *Statistical Mechanics* (Harper and Row, New York, 1976).
- [16] It is also possible to include a charge density term that accounts for one or many fixed macroions, such as the charged colloid particles studied in Refs. [1]–[5]. We will not consider this complication in the present work, because the system upon which we focus, a charged polymer in an electrolyte solution, is interesting in its own right.
- [17] The condition of ground state dominance is most readily realized when the polymer is confined by a potential (e.g., walls of a container), so that the energy spectrum of the Hamiltonian operator in Eq. (13) is discrete. The required condition is then $M(E_1 - E_0) \gg 1$, E_1 being the energy eigenvalue corresponding to the first excited state.
- [18] G.H. Golub and C.F. Van Loan, *Matrix Computations* (Johns Hopkins University, Baltimore, 1996).
- [19] W.H. Press, B.P. Flannery, S.A. Teukolsky, and W.T. Vetterling, *Numerical Recipes in C: The Art of Scientific Computing* (Cambridge University Press, Cambridge, 1992).
- [20] Note that according to the notational conventions established in Sec. II, χ_c [see Eq. (53)] is the *negative* of the standard electrical potential [21]. Thus $f(r)$ is large and positive near the negative charge source provided by the monomers of the polymer chain.
- [21] J.D. Jackson, *Classical Electrodynamics*, 2nd ed. (Wiley, New York, 1975).
- [22] S.A. Asher, J. Holtz, L. Liu, and Z. Wu, *J. Am. Chem. Soc.* **116**, 4997 (1994).
- [23] L. Liu, P. Li, and S.A. Asher, *J. Am. Chem. Soc.* **119**, 2729 (1997).
- [24] L. Liu, P. Li, and S.A. Asher, *Nature (London)* **397**, 141 (1999); L. Liu, P. Li, and S.A. Asher, *J. Am. Chem. Soc.* **121**, 4040 (1999).
- [25] E.F. Casassa, *Polym. Lett.* **5**, 773 (1967).
- [26] E.F. Casassa and Y. Tagami, *Macromolecules* **2**, 14 (1969).
- [27] A. Baumgärtner and M. Muthukumar, *J. Chem. Phys.* **87**, 3082 (1987).
- [28] M. Muthukumar and A. Baumgärtner, *Macromolecules* **22**, 1937 (1989).